We are IntechOpen, the world's leading publisher of Open Access books Built by scientists, for scientists

4,800
Open access books available

122,000
International authors and editors

135M
Downloads

Our authors are among the

154
Countries delivered to

TOP 1%
most cited scientists

12.2%
Contributors from top 500 universities

CLARIVATE ANALYTICS BOOK CITATION INDEX INDEXED

WEB OF SCIENCE™

Selection of our books indexed in the Book Citation Index in Web of Science™ Core Collection (BKCI)

Interested in publishing with us?
Contact book.department@intechopen.com

Numbers displayed above are based on latest data collected.
For more information visit www.intechopen.com

5

Physical Nature of "Slow Light" in Stimulated Brillouin Scattering

Valeri I. Kovalev[2], Robert G. Harrison[1] and Nadezhda E. Kotova[2]
[1]*Department of Physics, Heriot-Watt University, Edinburgh,*
[2]*PN Lebedev Physical Institute of the Russian Academy of Sciences, Moscow,*
[1]*UK*
[2]*Russia*

1. Introduction

It is well known that the velocity of a light pulse in a medium, referred to as the group velocity, is smaller than the phase velocity of light, c/n, where c is the speed of light in vacuum, and n is the refractive index of the medium. The difference between phase and group velocity of light is a result of two circumstances: a pulse is generically composed of a range of frequencies, and the refractive index, n, of a material is not constant but depends on the frequency, ω, of the radiation, $n = n(\omega)$. A group index $n_g(\omega) = n + \omega(dn/d\omega)$ is used to quantify the delay (or advancement), Δt_g, of an optical pulse, $\Delta t_g = n_g L/c$, which propagates in a medium of length L, where c/n_g is called the group velocity (Brillouin, 1960).
For about a century studies of this phenomenon, now topically referred to as slow light (SL), were mostly of a scholastic nature. In general the effect is very small for propagation of light pulses through transparent media. However when the light resonantly interacts with transitions in atoms or molecules, as for gain and absorption, the effect is greatly enhanced. Fig. 1 shows the gain (inverted absorption) spectral profile around a resonance together with its refractive index dispersion profile, the gradient of which results in $n_g(\omega)$.

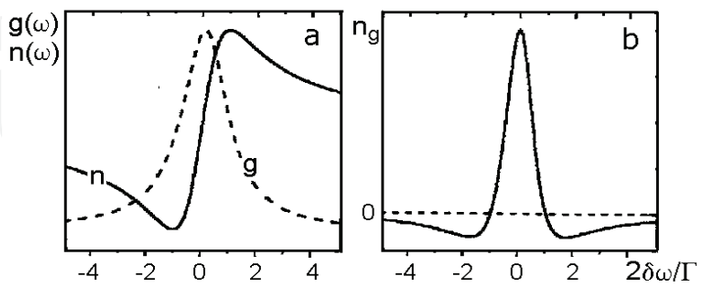

Fig. 1. a), Normalized dispersion of the gain coefficient, $g(\omega)$, (dashed line), the refractive index, $n(\omega)$, and b),the group index, $n_g(\omega)$, for a gain resonance.

As seen in the figure $n_g(\omega)$ peaks at line centre and it is here that the group delay is a maximum. However in reality for a meaningful delay the gain required must be high and this leads to competing nonlinear effects, which overshadow the slowing down (Basov et al., 1966). On the other hand in the vicinity of an absorbing resonance the corresponding

Source: Frontiers in Guided Wave Optics and Optoelectronics, Book edited by: Bishnu Pal,
ISBN 978-953-7619-82-4, pp. 674, February 2010, INTECH, Croatia, downloaded from SCIYO.COM

absorption is much too high to render the group effect useful. An exciting breakthrough happened in the early nineties when it was shown that group velocities of few tens of meters per second were possible with *nonlinear* resonance interactions (Hau et al., 1999). Two important features of nonlinear resonances make this possible: substantially reduced absorption, or even amplification, of radiation at a resonance, and sharpness of such resonances; the sharper a resonance, the higher $dn/d\omega$ and so the stronger the enhancement of group index, and hence the greater the pulse is delayed.

Widely ranging applications for slow light have been proposed, of which those for telecommunication systems and devices (optical delay lines, optical buffers, optical equalizers and signal processors) are currently of most interest (Gauthier, 2005). The essential demand of such devices is compatibility with existing telecommunication systems, that is they must be of wide enough bandwidth (≥10 GHz) and able to be integrated seamlessly into such systems.

Of the various nonlinear resonance mechanisms and media, which allow sufficiently long induced delays, stimulated Brillouin and Raman scattering (SBS and SRS) in optical fiber are deemed to be among the best candidates. Currently SBS is the most actively investigated and many experimental and theoretical papers on pulse delaying via SBS in optical fiber have been published in the last few years, see the review paper (Thevenaz, 2008) and references therein. In this process the pulse to be delayed is a frequency down-shifted (Stokes) pulse. This is transmitted through an optical fiber through which continuous wave (CW) pump radiation is sent in the opposite direction to prime the delay process. It is supposed that the Stokes pulse is amplified by parametric coupling with the pump wave and a material (acoustic) wave in the medium (Kroll, 1965), and the amplification is characterised by a resonant-type gain profile. The dispersion of refractive index associated with this profile (which is similar to that in Fig.1) can then be used to increase the group index for optical pulses at the Stokes frequency (Zeldovich, 1972).

Along with obvious device compatibility, there are several other advantages of the SL via SBS approach for optical communications systems: slow-light resonance can be created at any wavelength by changing the pump wavelength; use of optical fibre allows for long interaction lengths and thus low powers for the pump radiation, the process runs at room temperature, it uses off the shelf telecom equipment, and SBS works in the entire transparency range of fibers and in all types of fiber. Currently a main obstacle to applications of this approach is the narrow SBS gain spectral bandwidth, (Thevenaz, 2008), which is typically ≈ 120-200 MHz in silica fiber in the spectral range of telecom optical radiation (~1.3-1.6 μm) (Agrawal, 2006).

This chapter reviews our ongoing work on the physical mechanisms that give rise to pulse delay in SBS. In section 2 the theoretical background of the SBS phenomenon is given and the main working equations describing this nonlinear interaction are presented. In section 3 ways by which the SBS spectral bandwidth may be increased are addressed. Waveguide induced spectral broadening of SBS in optical fibre is considered as a means of increasing the bandwidth to the multi-GHz range. An alternative way widely discussed in the literature, (Thevenaz, 2008), is based on spectral broadening of the pump radiation. However it is shown through analytic analysis of the SBS equations converted to the frequency domain that pump radiation broadening by any reasonable amount has only a negligible effect on increasing the SBS bandwidth. Importantly in this section we show that, irrespective of the nature of the broadening considered, the SBS gain bandwidth remains

centred at the Brillion frequency which is far removed from the centre frequency of the Stokes pulse. Consequently the associated group index, which is enhanced at and around the SBS gain centre, cannot lead to group index induced delay of a Stokes pulse as claimed in the literature (Thevenaz, 2008). In section 4 the actual physical mechanisms by which a Stokes pulse is delayed through SBS are examined. Analytical analysis of the equations in the time domain shows that the SBS amplification process does not amplify an external the Stokes pulse and so again cannot induce group delay of this pulse. Rather the delay is shown to be predominantly a consequence of SBS gain build-up determined by inertia of the acoustic wave excitation. Finally in section 5 conclusions are drawn from this work in regard to current understanding of SL in SBS.

2. Theory of stimulated Brillioun scattering

In SBS, the resonance in a medium's response occurs at the Brillouin frequency, Ω_B, which is the central frequency of the variation of density in a medium, $\delta\rho(z,t) = 1/2\{\rho(z,t)\exp[-i(\Omega_B t+qz)] + \text{c.c.}\}$. This density variation is resonantly induced by an electrostrictive force resulting from interference of two plane counter-propagating waves, the forward-going ($+z$ direction) Stokes and backward-going ($-z$ direction) pump optical fields, $E_S(z,t) = 1/2\{E_S(z,t)\exp[-i(\omega_S t-k_S z)] + \text{c.c.}\}$ and $E_p(z,t) = 1/2\{E_p(z,t)\exp[-i(\omega_p t+k_p z)] + \text{c.c.}\}$, respectively, where $\rho(z,t)$, $E_S(z,t)$ and $E_p(z,t)$ are the amplitudes of the acoustic wave and of Stokes and pump fields, with $\Omega = \omega_p - \omega_S$ and $q = k_p + k_S$, ω_S and k_S, and ω_p and k_p being their radian frequencies and wavevectors and c.c. is the abbreviation for complex conjugate. In an isotropic medium $\delta\rho(z,t)$ is described by the equation, (Zeldovich et al., 1985),

$$\frac{\partial^2\delta\rho}{\partial t^2} - v_s^2\nabla^2\delta\rho - A\nabla^2\frac{\partial\delta\rho}{\partial t} = -\rho_0\frac{\partial\varepsilon}{\partial\rho}\frac{1}{16\pi}\nabla^2\left|\mathrm{E}(z,t)\right|^2, \tag{1}$$

where v_s is the speed of a free acoustic wave, A is its damping parameter, $\nabla^2 \equiv \partial^2/\partial z^2$ in the chosen plane wave model, ε and ρ_0 are the dielectric function and equilibrium density of the medium, and $E(z,t) = E_p(z,t) + E_S(z,t)$. Since the amplitude $\rho(z,t)$ is supposed to be slowly varying in space, then $\nabla^2\delta\rho(z,t) \cong -q^2\delta\rho(z,t)$ and Eq.(1) is usually reduced to

$$\frac{\partial^2\delta\rho}{\partial t^2} + \Omega_B^2\delta\rho + \frac{\Gamma_B}{2}\frac{\partial\delta\rho}{\partial t} = -\rho_0\frac{\partial\varepsilon}{\partial\rho}\frac{1}{8\pi}\frac{\partial^2}{\partial z^2}\left[\mathrm{E}_p(z,t)\mathrm{E}_S(z,t)\right]. \tag{2}$$

This is then the equation for the induced acoustic wave. It is a typical equation for an externally driven damped resonant oscillator, in which the right-hand side is the driving force, $\Omega_B = qv_s = 2v_s\omega_p/(c/n+v_s) \cong 2nv_s\omega_p/c$ is the resonant frequency of the oscillator, known as the Brillouin frequency, Γ_B is the FWHM spectral width of the resonant profile with $2/\Gamma_B$ being the decay time of the acoustic wave.

The pump field reflected by the induced acoustic wave is a new Stokes field, which in turn interacts with the pump field to further electrostrictively enhance the acoustic wave and so the Stokes field and so forth. Increase of the Stokes field in SBS is therefore a direct consequence of increase of reflectivity of the acoustic wave for the pump field. As such, so called "SBS gain" characteristics are determined by the reflectivity, spectral characteristics and dynamics of the acoustic wave. In the approximation that the CW pump radiation is not

depleted over the interaction length, L, the spatial/temporal evolution of the Stokes signal is described by the nonlinear wave equation,

$$\frac{\partial^2 \mathrm{E}_S}{\partial z^2} - \frac{\varepsilon}{c^2}\frac{\partial^2 \mathrm{E}_S}{\partial t^2} = \frac{1}{c^2}\frac{\partial \varepsilon}{\partial \rho}\frac{\partial^2}{\partial t^2}\left[\delta\rho(z,t)\mathrm{E}_p(z,t)\right]. \tag{3}$$

Eqs (2) and (3) are the basic equations, which describes the SBS phenomenon in an optically lossless medium in the small signal plane wave approximation. Since the density and Stokes field amplitudes, $\rho(z,t)$ and $E_S(z,t)$, vary slowly in both space and time and the acoustic wave in SBS attenuates strongly, their evolution is usually reduced to two well known first order equations: from Eq.(2) the relaxation equation for $\rho(z,t)$,

$$\frac{\partial \rho}{\partial t} + \left(\frac{\Gamma_B}{2} + i\delta\Omega\right)\rho = -i\rho_0 \frac{\partial \varepsilon}{\partial \rho}\frac{\Omega_B}{8\pi v_s^2} E_p(t)E_S^*(z,t)\,, \tag{4}$$

which describes the amplitude of the driven damped resonant oscillator, and from Eq.(3) the partial differential equation for $E_S(z,t)$,

$$\frac{\partial E_S}{\partial z} + \frac{n}{c}\frac{\partial E_S}{\partial t} = -i\frac{\omega_S}{2cn}\frac{\partial \varepsilon}{\partial \rho}\rho^*(z,t)E_p(t)\,. \tag{5}$$

Here $\delta\Omega = \Omega - \Omega_B$ is the difference between the acoustic drive frequency, Ω, and the resonant Brillouin frequency and asterisk, *, marks complex conjugate. The right-hand side of Eq. (5) is a source of the Stokes emission.

3. Spectral broadening of SBS

In the literature on group index induced slow light it is argued that rate at which optical pulses may be delayed is ultimately determined by the spectral bandwidth of the resonance responsible for slow light generation in the material (Boyd & Gauthier, 2002). So, the narrower the bandwidth the larger is the delay. On the other hand, to minimize pulse distortion the bandwidth must exceed substantially that of the optical pulse to be delayed and consequently determines a lower limit for the duration of the optical pulse. This argument is correct for systems in which a resonance in the material is in resonance with the optical pulse to be delayed, such as those based on electromagnetically induced transparency and coherent population oscillation (Boyd & Gauthier, 2002). However as shown below this does not apply to SBS since the resonance occurs around the Brillouin frequency, Ω_B, which is far from the frequency of the Stokes pulse to be delayed. This point has been overlooked in the literature on SL via SBS and as a consequence has led to misinterpretation of experimental findings of Stokes pulse delay in SBS. This issue is considered in some detail in section 4 where it is shown the Stokes delay arises from the inertial build up time of SBS and not group index delay as has been claimed throughout the literature. Nevertheless it is still of academic interest to consider ways in which the spectral bandwidth of SBS may be increased and this is considered below.

The physical mechanism responsible for Γ_B is attenuation of the Brillioun acoustic wave, in liquids and solid optical media this is predominantly due to viscosity (Zeldovich et al., 1985). Such spectral broadening is homogeneous in nature. For bulk silica, Γ_B, scales with

pump radiation wavelength, λ, as $\Gamma_B \cong 2\pi 40/\lambda^2$ MHz (Heiman et al. 1979), where λ is in μm. It is evident from this expression that the shorter the radiation wavelength the wider the spectrum, so for radiation in the short wavelength transmission window of silica, λ ≅ 0.2 μm, Γ_B is expected to be ~2π GHz compared to ~ 20 MHz at telecom wavelengths, λ ≅ 1.3-1.6 μm. The SBS gain bandwidth in fibers may also be broadened through varying fiber design, doping concentration, strain and/or temperature (Tkach et al., 1986; Shibata et al., 1987; Azuma et al., 1988; Shibata et al., 1989; Yoshizawa et al., 1991; Tsun et al., 1992; Yoshizawa & Imai, 1993; Shiraki et al., 1995; LeFloch & Cambon, 2003). However the highest achieved line-width enhancement factor, compared to Γ_B is ~5, (Yoshizawa et al., 1991). A potentially attractive solution to increasing Γ_B is by waveguide induced spectral broadening (Kovalev & Harrison, 2000), which is discussed in some detail below (Sect. 3.1). Spectral broadening of the pump radiation has also been proposed (Stenner et al., 2005, Herraez et al., 2006) as a means for broadening Γ_B and is currently a subject of considerable activity (Thevenaz, 2008). However, as shown below (see Sect. 3.2) the effect is in fact negligible.

3.1 Waveguide induced spectral broadening of SBS

Due to the waveguiding nature of beam propagation in optical fiber and its effect on the SBS interaction, such propagation has been shown to render the Stokes spectrum inhomogeneous (Kovalev & Harrison, 2000), the bandwidth of which is massive in fibers of high numerical aperture, NA (Kovalev & Harrison, 2002). The nature of the broadening arises from the ability of optical fiber to support a fan of beam directions within an angle $2\theta_c$ (Fig. 2), where θ_c is the acceptance angle of the fiber, defined as

$$\theta_c = \arcsin\left\{1 - \frac{n_{cl}^2}{n_{co}^2}\right\}^{1/2} = \arcsin\left[\frac{NA}{n_{co}}\right], \tag{6}$$

where $n_{cl,co}$ are the refractive indices of the fiber cladding and core, respectively.

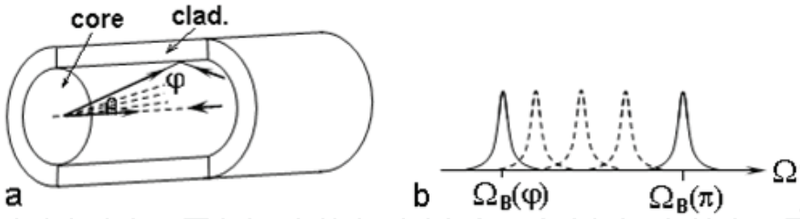

Fig. 2. Sketch showing the nature of waveguide induced broadening of SBS gain spectrum; a), schematic of fiber, and, b), homogeneously broadened spectral profiles for different angles of scattering, φ.

The frequency shift of the Stokes depends on the angle, φ, between the momentum vectors of the pump and scattered radiation through the relation $\Omega_B(\varphi)=4\pi n v_s \sin(\varphi/2)/\Lambda$. So the range of $\Omega_B(\varphi)$ in a fiber will be from $\Omega_B(\pi) = 4\pi n v_s/\Lambda$ to $\Omega_B(\pi-2\theta_c) = 4\pi n v_s \cos\theta_c/\Lambda$. For every $\Omega_B(\varphi)$ there corresponds a homogeneously broadened line of the form

$$\gamma_h(\Omega, \Omega_B) = \left[\frac{\Gamma_B^2}{4(\Omega_B - \Omega)^2 + \Gamma_B^2}\right]. \tag{7}$$

The Stokes spectrum, broadened by guiding, is then the convolution of frequency-shifted homogeneously broadened components, each generated from a different angular component of the pump and Stokes signal (such broadening is inhomogeneous by definition). The shape of the broadened Brillouin linewidth is described by the equation (Kovalev & Harrison, 2002),

$$\gamma_i(\Omega,\theta_c)=\frac{\Gamma_B}{2\left[\Omega_B(\pi)-\Omega_B(\pi-2\theta_c)\right]}\left[\tan^{-1}\left(2\frac{\Omega_B(\pi)-\Omega}{\Gamma_B}\right)-\tan^{-1}\left(2\frac{\Omega_B(\pi-2\theta_c)-\Omega}{\Gamma_B}\right)\right], \tag{8}$$

where θ_c is linked to NA through Eq.(6). Fig. 3 shows $\gamma_i(\Omega,\theta_c)$ for five values of NA.

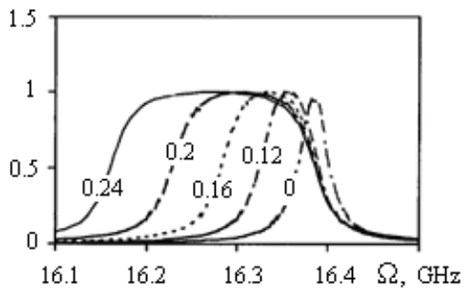

Fig. 3. Line shape of the Brillouin gain spectrum in optical fiber for several NA values (Kovalev & Harrison, 2002).

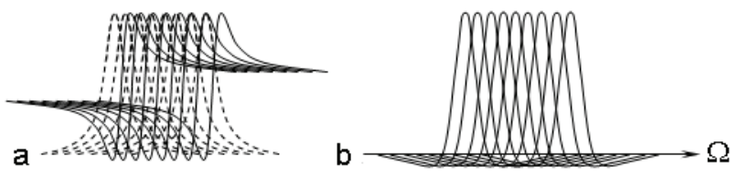

Fig. 4. Relation between, a), the gain profile (dashed) and the phase index (solid) and, b), group index, for SBS in optical fibers.

Intuitively, the dispersion and group index profiles, which are associated with the convolutionally broadened SBS gain spectrum (dashed lines in Fig.4a), are expected to also be convolutionally broadened (solid lines in Fig.4a and Fig.4b). As seen (Fig.4b) the maximum n_g is expected to be more or less constant and so it's value for each and all the homogeneous spectral components that contribute to the group index profile is the same.
The shape of the group index spectrum is determined more precisely by numerical simulation (Kovalev et al., 2008). The group index in the case of the SBS resonance in optical fiber can be expressed as (Okawachi, 2005; Kovalev & Harrison, 2005),

$$n_g(\Omega_B,\Omega)=n-\frac{g_0 I_p \lambda \Gamma_B}{2\pi}\left\{\frac{(\Omega_B-\Omega)}{4(\Omega_B-\Omega)^2+\Gamma_B{}^2}+\omega\frac{4(\Omega_B-\Omega)^2-\Gamma_B{}^2}{\left[4(\Omega_B-\Omega)^2+\Gamma_B{}^2\right]^2}\right\}, \tag{9}$$

where g_0 is the value of the SBS gain coefficient at the exact Brillouin resonance and I_p is the pump radiation intensity. When several resonant frequencies, Ω_B, exist in the medium, and the distribution of their relative amplitudes over the range from $\Omega_B(\pi)$ to $\Omega_B(\pi\text{-}2\theta_c)$ is some

function $F(\Omega_B)$, the spectrum of the "broadened" group index, $n_{gb}(\Omega)$, is described by the convolution integral,

$$n_{gb}(\Omega) = \int_{\Omega_B(\pi-2\theta_c)}^{\Omega_B(\pi)} F(\Omega_B) n_g(\Omega_B, \Omega) d\Omega_B \,. \tag{10}$$

Results of calculations for the case when $F(\Omega_B) = 1$ in the range from $\Omega_B(\pi)$ to $\Omega_B(\pi\text{-}2\theta_c)$ are presented in Fig.5. For the sake of illustration the results are centred by shifting the limits of integration in such a way that the lower limit is $\omega_1 = \omega_0 - m\Gamma_B/2$ and $\omega_2 = \omega_0 + m\Gamma_B/2$, where m, which is called the rate of broadening, varies from 2 to 100. As seen the width of the profile increases continuously with increasing m. The original shape of the profile (individual components in Fig 4b) is retained for a broadening of $m \leq 2$. Beyond this, the profile becomes top-hat, at $m \cong 4$, and for $m > 4$ it exhibits a dip, the depth of which increases with increasing m. For $m > 20$ the dip tends to becomes flat-bottomed. It can therefore be seen that the value of group index can stay constant over a broad range of frequencies, especially when $m > 60$. However the price for this is a reduced magnitude of the group index. However, as seen in Eq.(9), this may be compensated for by increase of the pump intensity.

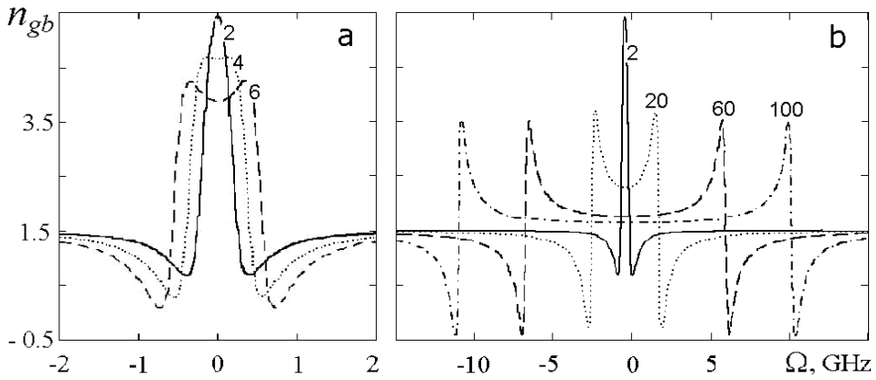

Fig. 5. Shape of group index, n_{gb}, spectrally broadened due to waveguiding nature of fiber, a) for m = 2-6, and b), for m = 2-100.

Earlier work has shown that waveguide induced broadening is dependant on the numerical aperture of fiber through the equation (Kovalev & Harrison, 2002),

$$\Gamma \cong \sqrt{\Gamma_B^2 + \Omega_B^2 \frac{(NA)^4}{4n_{co}^4}} \,. \tag{11}$$

It follows from Eq.(11) that in the calculations above, m = 2 corresponds to NA = 0.12, which is standard for single-mode telecom fiber. However, it is now readily possible to realise single-mode fiber with much higher NA, ~0.8 (Knight et al., 2000). For such fiber the broadening is ~15 GHz, which is comparable with the needs of telecom devises. As noted above this analysis assumes that the homogeneously broadened Brillouin gain contributions to the inhomogeneous profile are uniformly distributed, $F(\Omega_B) = 1$. It is relatively straight forward to account for alternative distributions by introducing their appropriate shape function $F(\Omega_B)$ into Eq.(10).

These considerations therefore show that waveguide induced spectral broadening of the gain bandwidth of SBS in optical fiber is potentially massive (> 10 Gb/s), and readily achievable.

3.2 On the effect of the pump spectral width on spectral broadening of SBS

It has been proposed in (Stenner et al., 2005) that spectral broadening of the pump radiation may lead to comparable spectral broadening of the Stokes pulse in SBS. This approach has since been the focus of many publications, (Minardo et al., 2006; Shumakher et al., 2006; Zhu & Gauthier, 2006; Zadok et al., 2006; Chin et al., 2006; Schneider et al., 2006; Kalosha et al., 2006; Zhu et al., 2007; Song & Hotate, 2007; Lu et al., 2007; Zhang et al., 2007-1 & -2; Yi et al., 2007; Shi et al., 2007; Pant et al., 2008; Ren & Tomita, 2008; Sakamoto et al., 2008; Wang et al., 2008; Schneider et al., 2008; Cheng et al., 2008), aimed at high data rate applications of SL. In this section the validity of this assertion is examined and it is shown that the effect is in fact negligible.

This may be seen from examining the spectral features of the medium's response and the Stokes emission through Fourier transformation of Eqs (4) and (5) using the following basic properties of Fourier transforms, $F(\omega) \equiv S[f(t)]$, (Korn & Korn, 1967),

$$S[f(t)] = \int_{-\infty}^{\infty} f(t)e^{-i\omega t}dt,\ S[\frac{d}{dt}f(t)] = i\omega S[f(t)],\ \ and\ \ S[f_1(t)f_2(t)] = \frac{1}{2\pi}\int_{-\infty}^{\infty} F_1(\nu)F_2(\omega-\nu)d\nu\ , \quad (12)$$

where $f(t)$ is a function of time. Here ω and ν are Fourier transform frequencies, which are the difference frequencies of the acoustic, Stokes and pump signals from their respective line centers. Eqs (4) and (5) then give

$$\left(\frac{\Gamma_B}{2} - i(\omega + \delta\Omega)\right)\tilde{\rho}^*(z,\omega) = i\rho_0\frac{\partial\varepsilon}{\partial\rho}\frac{\Omega_B}{8\pi v_s^2}\frac{1}{2\pi}\int_{-\infty}^{\infty}\tilde{E}_p'^*(\nu)\tilde{E}_S'(z,\omega-\nu)d\nu\ , \quad (13)$$

and

$$\frac{d\tilde{E}_S(z,\omega)}{dz} + i\omega\frac{n}{c}\tilde{E}_S(z,\omega) = -i\frac{\omega_S}{2cn}\frac{\partial\varepsilon}{\partial\rho}\frac{1}{2\pi}\int_{-\infty}^{\infty}\tilde{E}_p(\nu)\tilde{\rho}^*(z,\omega-\nu)d\nu\ . \quad (14)$$

Note that here we have primed the Stokes and pump fields within (13), which are responsible for inducing the acoustic wave, to distinguish them from the generated Stokes field, (LHS of (14)), and from the pump field, which generates the new Stokes field, (the field $\tilde{E}_p(\omega)$ under the integral in (14)). $\delta\Omega$ is a detuning parameter, which can influence only the strength of the medium's response to the drive force at frequency, Ω. (In the case of non-monochromatic pump and Stokes fields $\delta\Omega$ can be considered as the difference between the central frequencies of their bandwidths.)

Consider the case of a typical SBS slow light experiment in which the spectrum of the Stokes signal corresponds to that of a temporally smooth pulse and the spectrum of the pump radiation is the Fourier-transform of a continuous wave field the amplitude of which is randomly fluctuating in time. As seen, the right-hand sides of these equations are proportional to the convolution integrals of spectra $\tilde{E}_p'^*(\omega)$ and $\tilde{E}_S'(z,\omega)$ in Eq.(13), and $\tilde{E}_p(\omega)$ and $\tilde{\rho}^*(z,\omega)$ in Eq.(14), respectively.

Eq. (13) is an algebraic equation, the solution of which gives the spectrum of the medium's response

$$\tilde{\rho}^*(z,\omega) = i\rho_0 \frac{\partial\varepsilon}{\partial\rho}\frac{\Omega_B}{8\pi v_s^2}\frac{F_\rho(z,\omega)}{\left(\Gamma_B/2 - i(\omega+\delta\Omega)\right)}, \tag{15}$$

where

$$F_\rho(z,\omega) = \frac{1}{2\pi}\int_{-\infty}^{\infty}\tilde{E}_p^{'*}(\nu)\tilde{E}_S^{'}(z,\omega-\nu)d\nu \tag{16}$$

is the function which determines the spectrum of the driving force for the medium's response. The spectrum of the medium's response is then given by the modulus of $\tilde{\rho}^*(z,\omega)$, $\left|\tilde{\rho}(z,\omega)\right|$.

The spectrum of the Stokes field is described by the first order differential equation, Eq.(14), the solution of which is

$$\left|\tilde{E}_S(z,\omega)\right| = \left|e^{-i\frac{\omega n}{c}z}\left[\tilde{E}_S(0,\omega) + i\frac{\omega_S}{2nc}\frac{\partial\varepsilon}{\partial\rho}\int_0^z F_E(x,\omega)e^{i\frac{\omega n}{c}x}dx\right]\right|, \tag{17}$$

where $\tilde{E}_S(0,\omega)$ is the spectrum of an input Stokes signal at z = 0 and

$$F_E(z,\omega) = \frac{1}{2\pi}\int_{-\infty}^{\infty}\tilde{E}_p(\nu)\tilde{\rho}^*(z,\omega-\nu)d\nu \tag{18}$$

is the function which determines the spectrum of the source of the generated Stokes field. Equations (15)-(18) describe the spectral features of the SBS-induced material response and Stokes field when both optical fields, pump and Stokes, are non-monochromatic. Note that solution Eq.(17) in the *spectral* domain is entirely consistent with the analytical solution of Eqs. (4) and (5), previously obtained in the *temporal* domain for stimulated scattering induced by non-monochromatic pump and monochromatic Stokes fields in (Kroll, 1965, Charman et al., 1970, Akhmanov et al., 1971, Akhmanov et al., 1988), and for monochromatic pump and non-monochromatic Stokes fields in (Kovalev et al., 2009).

It is easily seen that the solution (17) for the Stokes field differs substantially from that usually deduced in textbooks from (4) and (5) in the steady state approximation (that is when both pump and Stokes fields are considered *monochromatic*),

$$E_S(z) = E_S(0)e^{\frac{g_0\left|E_pE_p^*\right|z}{2(1-i2\delta\Omega\Gamma_B^{-1})}}, \tag{19}$$

which results from the equation for the Stokes field of the form, (Zeldovich et al., 1985),

$$\frac{dE_S(z)}{dz} = \left[\frac{g_0\left|E_pE_p^*\right|}{2(1-i2\delta\Omega\Gamma_B^{-1})}\right]E_S(z). \tag{20}$$

Here it is again important to remember that δΩ is a detuning parameter, the value of which is the difference between the frequencies of the monochromatic pump and Stokes fields as

chosen, $\Omega = \omega_p - \omega_S$, and the resonant Brillouin frequency, Ω_B, $|E_pE_p^*|$ is the pump radiation intensity, and g_0 is the standard steady state SBS gain coefficient. Equation (20) means that the Stokes field is amplified in the medium with gain proportional to the pump radiation intensity. To appreciate the difference between this case and our case let us consider both pump and Stokes fields in Eqs.(13)-(18) to be *monochromatic*. The spectra of the amplitudes of driving forces and of the medium's response then reduce to δ-functions at $\omega = 0$ and these depend on z only. The equation for the Stokes field is then,

$$\frac{dE_S(z)}{dz} = \left[\frac{g_0(E_p^{*}E_S^{'}(z))}{2(1-i2\delta\Omega\Gamma_B^{-1})}\right]E_p\,, \tag{21}$$

The physical meaning of Eq.(21) is substantially different from that of Eq.(20), though their mathematical forms may look similar. Equation (21) describes the spatial evolution of the amplitude of the Stokes field, which results from reflection of the pump field by the induced acoustic wave. Since the Stokes field on the RHS of Eq.(21) is responsible for creating the acoustic wave, it is not the same as the reflected Stokes field on the LHS of this equation and therefore it is distinguished by its prime. Though for this monochromatic case the Stokes fields have the same frequency, their roles still remain physically distinct as in our general treatment above. Such distinction is not made in the text-book treatment that leads to Eq.(20) and to its familiar exponential solution, Eq.(19), which displays "gain" and a "modified propagation constant" for the Stokes field (see (Zhu et al., 2005)). Evidently the solution for Eq.(21) cannot be the same. As such, though the RHS of this equation has both real and imaginary parts (in the case of non-zero detuning, δΩ), this does not modify the propagation constant for the reflected Stokes field and therefore it can have no bearing on changing the refractive and group index for this field.

Returning now to the solutions (15)-(18) of Eqs. (13) and (14) for the general case in which either one of the fields or both have nonzero bandwidth, they display three important features of the SBS interaction: i) the external input Stokes signal, as seen in Eq.(17), propagates through a non-absorbing medium without gain or measurable loss (its energy loss for creating the acoustic wave is usually negligible), ii) the SBS-generated Stokes signal is a result of reflection of the pump radiation by the acoustic wave, which is created by the pump and the original Stokes fields (see Eqs. (4) and (5)), and iii) each spectral component of the generated Stokes signal arises from a range of spectral components of the non-monochromatic pump and Stokes fields, see Eqs. (17) and (18).

To see the consequences of this, consider the case when the growth of the Stokes field along z is small. As such, the z dependence of $\tilde{E}_S(z,\omega)$ and $\tilde{\rho}^*(z,\omega)$ is dropped. While this approximation does not account for gain narrowing of the SBS spectrum, typical for higher amplification, (Zeldovich et al., 1985), it still captures reasonably well the trends in the spectral features of the Stokes field, $\tilde{E}_S(z,\omega)$, the medium response, $|\tilde{\rho}(\omega)|$, and so the SBS gain and the modified refractive and group indices. It then follows from Eq.(17) that the output spectrum of the Stokes signal, $|\tilde{E}_S(\omega)|$, is the sum of the Fourier spectra of the input Stokes signal, $|\tilde{E}_S(0,\omega)|$, and the convoluted spectrum of the pump field and medium's excitation, characteristics which are described by the function $F_E(\omega)$ (see Eq. (18)). The latter is the SBS-induced contribution to the Stokes signal, and is determined by which of $\tilde{E}_p(\omega)$ or $\tilde{\rho}^*(\omega)$ is spectrally broadest. These spectral features of the output Stokes radiation are

consistent with those predicted earlier in the low gain approximation using the *temporal* domain treatment of stimulated Raman scattering, (Akhmanov et al., 1971, Akhmanov et al., 1988), and SBS, (Zeldovich et al., 1985), with non-monochromatic pump fields.

In contrast to the spectral features of the Stokes emission, those of the medium's response, $|\tilde{\rho}(\omega)|$, have to date received little attention. According to Eq.(15) this case is not as straightforward as that of the Stokes spectrum since a Lorentzian shape multiplier of bandwidth Γ_B appears in addition to the convolution integral, $F_\rho(\omega)$. From Eq. (15), $|\tilde{\rho}(\omega)|$ is given as

$$|\tilde{\rho}(\omega)| = \rho_0 \frac{\partial \varepsilon}{\partial \rho} \frac{\Omega_B}{8\pi v_s^2} \frac{|F_\rho(\omega)|}{\sqrt{\Gamma_B^2/4 + (\omega + \delta\Omega)^2}}. \tag{22}$$

Examples of the spectra, $|\tilde{\rho}(\omega)|$, are shown in Fig. 6 by solid curves for δΩ = 0 (Fig. 6(a)) and δΩ = 0.1 GHz (Fig. 6(b)).

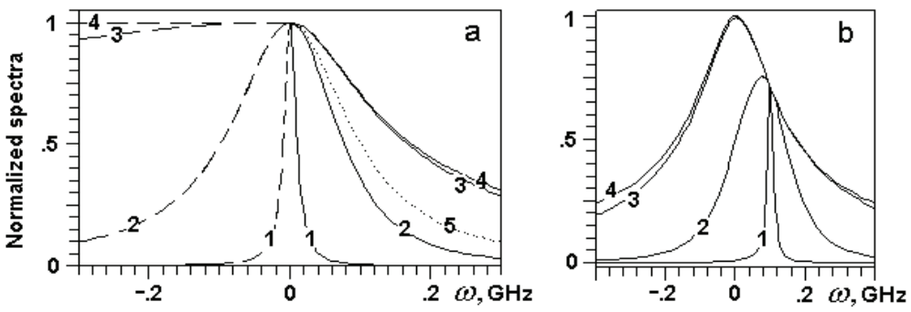

Fig. 6. a), LHS and RHS halves of the (symmetrical) spectra of $|F_\rho(\omega)|$ (dashed) and of $|\tilde{\rho}(\omega)|$ (solid lines) respectively for spectral widths of $F_\rho(\omega)$ 0.02(1), 0.2(2), 2(3) and 20(4) GHz, when Γ_B = 0.2 GHz and δΩ = 0. The dotted line 5 is the Lorentzian-shaped spectrum with Γ_B = 0.2 GHz; b), spectra of $|\tilde{\rho}(\omega)|$ for the same spectral widths of $F_\rho(\omega)$ when δΩ = 0.1 GHz.

It follows from Eq.(22) that when the spectral width, $\delta\omega_\rho$, of the driving force, $|F_\rho(\omega)|$ (shown by dashed curves in Fig. 6(a)), is narrower than Γ_B, the width, Γ, and centre frequency of $|\tilde{\rho}(\omega)|$ is determined by $|F_\rho(\omega)|$, (the convolution of $\tilde{E}_p^*(\omega)$ and $\tilde{E}_S(\omega)$ as given in Eq. (16)), the central frequency of which is detuned by δΩ as shown by curve 1 in Fig. 6(b). Nonzero detuning δΩ results also in decreased amplitude of the medium's response (compare solid curves 1 of Figs. 6(a) and 6(b)). As $\delta\omega_\rho$ increases, Γ grows and for $\delta\omega_\rho > \Gamma_B$ it saturates at ~1.7Γ_B (solid curves 3 and 4 in Fig. 6(a)), and the effect of the detuning δΩ on the features of the medium's spectrum becomes negligible (compare solid curves 3 and 4 in Figs. 6(a) and 6(b)). In essence, this means that irrespective of how broad the bandwidth of the broadband pump and/or Stokes emission is/are, the bandwidth of the material response spectrum is predominantly determined by the features of the material and can never be much greater than that of the medium's resonant response (~Γ_B). This is exactly the features expected from an externally driven damped resonant oscillator (see Eq.(2)).

From Eq. (22) the SBS induced dispersion of refractive index, $\Delta n(\omega) \cong (\partial\varepsilon/\partial\rho)\,|\,\tilde{\rho}(\omega)\,|/2n_0$, and its corresponding induced group index at the frequency of the Stokes radiation, $n_g(\omega_S) = n_0(\omega_S) + \omega_S(d\Delta n/d\omega)|_{\omega_S}$, may be directly determined. To do so let us replace the relative frequency ω in the equations above with the absolute frequency, ω', and consider the spectrum of $|F_\rho(\omega')|$ to be Gaussian in shape centred at frequency Ω_B, $F_\rho(\omega') = F_{\rho a}\exp[-(\omega'-\Omega_B)^2/\delta\omega_\rho^2]$, where $F_{\rho a} = \sqrt{I_p I_S}$ is the spectral amplitude and I_S is the Stokes signal intensity. The induced group index at absolute frequency ω' is then

$$n_g(\omega') = -B\frac{\omega'(\omega'-\Omega_B)}{\delta\omega_\rho^2}\left[\frac{\Gamma_B^2}{2} + 2(\omega'-\Omega_B)^2 + \delta\omega_\rho^2\right]\left[\frac{\Gamma_B^2}{4} + (\omega'-\Omega_B)^2\right]^{-3/2} e^{-\frac{(\omega'-\Omega_B)^2}{\delta\omega_\rho^2}}, \quad (23)$$

where $B = \rho_0\left(\frac{\partial\varepsilon}{\partial\rho}\right)^2\frac{\Omega_B\sqrt{I_p I_S}}{16\pi n_0 v_s^2}$.

The dispersion of the SBS-induced group index, which is described by Eq. (23), has a maximum at $\omega' = \Omega_B - \Delta$ and a minimum at $\omega' = \Omega_B + \Delta$, where Δ is functionally dependent on $\delta\omega_\rho$ and is $< \Gamma_B/2$. These maximum and minimum, in principle, may be of very high amplitude, however it is critically important to note that they are located at $\omega' \approx \Omega_B$. At the Stokes frequency, $\omega' = \omega_S$, since $\omega_S >> \Omega_B > \Gamma_B$ ($\omega_S \approx 1.7\cdot10^4\Omega_B$ in silica), Eq.(23) reduces to

$$n_g(\omega_S) = -\frac{2B\omega_S}{\delta\omega_\rho^2}e^{-\frac{\omega_S^2}{\delta\omega_\rho^2}}, \quad (24)$$

which shows that the SBS-induced $n_g(\omega_S)$ is independent of both Γ_B and Ω_B, and is negligibly small for any reasonable bandwidth, $\delta\omega_\rho$, of $|\tilde{\rho}(\omega)|$. As such the acoustic resonance can have next to no effect in enhancing or modifying the natural group index in the medium for the Stokes signal. Consequently spectral broadening of pump radiation by any reasonable amount results in only minute increase of the spectral width of the material's resonant excitation in SBS, and furthermore because this resonance is far away from a Stokes optical signal frequency to be delayed the approach cannot be effective in modifying a natural group index of a medium.

This may also be seen using the following less rigorous simple argument. The resonant Brillouin frequency, Ω_B, that is the frequency of the acoustic wave, for Stokes radiation excited by a monochromatic pump radiation, is $\Omega_B = 2n\nu_s\omega_p/c$. Broadening of the pump radiation spectrum by $\Delta\omega_p$ then results in pump induced broadening of the acoustic wave spectrum, $\Delta\Omega_B$, $= 2n\nu_s\Delta\omega_p/c$. It follows that for $\Delta\omega_p$ of ~$2\pi\cdot$(12-25) GHz (Zu et al., 2007; Song & Hotate, 2007), which is of order of Ω_B for SBS excited by 1.55 μm pump radiation in silica fiber ($n \cong 1.45$, $\nu_s \cong 6$ km/s), $\Delta\Omega_B \cong 2\pi\cdot(0.6\text{-}1.5)$ MHz << $\Gamma_B \cong 2\pi\cdot16$ MHz. Clearly then pump induced broadening of the acoustic wave spectrum is negligible compared to its homogeneous spectral width, Γ_B, for any reasonable value of the pump spectrum width up to few tens of GHz.

4. Effect of acoustic wave inertia on Stokes pulse delay in SBS

In this section the underlying physical processes that give rise to Stokes pulse delay in SBS are addressed.

In typical SBS-based slow light experiments the CW pump power is kept below the value at which the SBS interaction experiences pump depletion. The pump power is therefore constant throughout the interaction length (in lossless media). This is also an underlying reason why the contribution of spontaneous scattering to the SBS interaction is considered sufficiently small to be ignored in theoretical treatments of this problem (Song et al., 2005; Okawachi et al., 2005; Zhu et al., 2005). Equations (4) and (5) with appropriate boundary conditions are therefore sufficient for describing the evolution of a Stokes pulse in a medium.

It is convenient to introduce the new temporal coordinate $t' = t - zn/c$ and suppose that the centre frequency of the Stokes pulse spectrum coincides with the resonant Brillouin Stokes frequency, that is $\delta\Omega = 0$. In terms of the new variables Eqs (4) and (5) can be rewritten as

$$-\frac{\partial E_S}{\partial z} = -i\frac{\omega_S}{2cn}\frac{\partial \varepsilon}{\partial \rho}(\rho(t')) * E_p\,, \tag{25}$$

and

$$\frac{\partial \rho}{\partial t'} + \frac{1}{\tau}\rho = -i\rho_0\frac{\partial \varepsilon}{\partial \rho}\frac{\Omega_B}{8\pi v_s^2}E_p E_S^*(t')\,. \tag{26}$$

This set of equations has an analytic solution, which can be obtained using Reimann's method (Bronshtein & Semendyaev, 1973). Consider the case addressed in typical SL experiments, in which the duration of the Stokes pulse is much less than its transit time in the medium and the pump is CW monochromatic radiation. Assuming that there are no acoustic waves in the medium before a Stokes pulse enters, and $E_S(t' \le 0) = 0$, $E_S(z=0,t') = E_{S0}(t')$ and $E_p(z,t') \equiv E_p = \text{const}$, the solutions for the Stokes field and the density variation are then

$$E_S(z,t') = E_{S0}(t') + \frac{g\mathrm{I}_p z}{\tau}\int_0^{t'}\left(e^{-\frac{t'-\vartheta}{\tau}}\right)I_1\left(\sqrt{2g\mathrm{I}_p z\frac{t'-\vartheta}{\tau}}\right)\sqrt{2g\mathrm{I}_p z\frac{t'-\vartheta}{\tau}}E_{S0}(\vartheta)d\vartheta \tag{27}$$

and

$$\rho(t') = -i\rho_0\frac{\partial \varepsilon}{\partial \rho}\frac{\Omega_B}{8\pi\tau v^2}E_p\int_0^{t'}\left(e^{-\frac{t'-\vartheta}{\tau}}\right)I_0\left(\sqrt{2g\mathrm{I}_p z\frac{t'-\vartheta}{\tau}}\right)E_{S0}^*(\vartheta)d\vartheta\,. \tag{28}$$

Here $\mathrm{I}_p = |E_p|^2$ is the pump radiation intensity in [W/cm^2], $I_{0,1}(x)$ are the Bessel functions of imaginary argument x, and g is the SBS gain coefficient,

$$g = 10^7\frac{\omega_S^2\rho_0\tau}{4nc^3v_s}\left(\frac{\partial \varepsilon}{\partial \rho}\right)^2\,[cm/W]\,. \tag{29}$$

Suppose that the input Stokes signal is an optical pulse, the time dependent intensity of which is given by

$$\mathrm{I}_S(z=0,t) = \left|E_S(z=0,t)\right|^2 = \mathrm{I}_{S0}(3.5t/t_p)^2 e^{-3.5t/t_p}\,, \tag{30}$$

where I_{S0} is the intensity at the peak of the pulse, t_p is the FWHM pulse duration. The shape of the pulse is shown in Figs. 7 and 8 (curves for G = gI_pL =0) and it is a good approximation for pulses actually used in experiments (Pohl & Kaiser, 1970). Since the SBS exponential gain, G, in the fiber is supposed to be below the SBS threshold, this, according to (Kovalev & Harrison, 2007), limits G to ≤12 for standard silica fibers of > 0.1 km length.

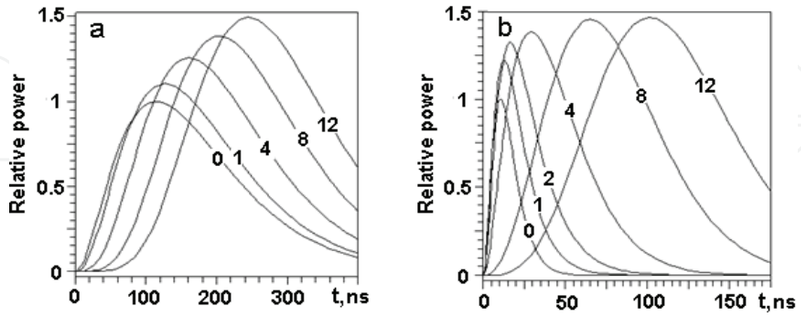

Fig. 7. Output Stokes pulse shapes for a), t_p = 200 ns (>>τ) and G = 0 (1), 1(0.42), 4(0.026), 8(0.0006), and 12(0.000012) and b), for t_p = 18 ns (=τ) and G = 0(1), 1(0.9), 2(0.6), 4(0.2), 8(0.09), and 12(0.00026), where numbers in brackets are the amplitude magnification factors. The numbers on curves are Gs.

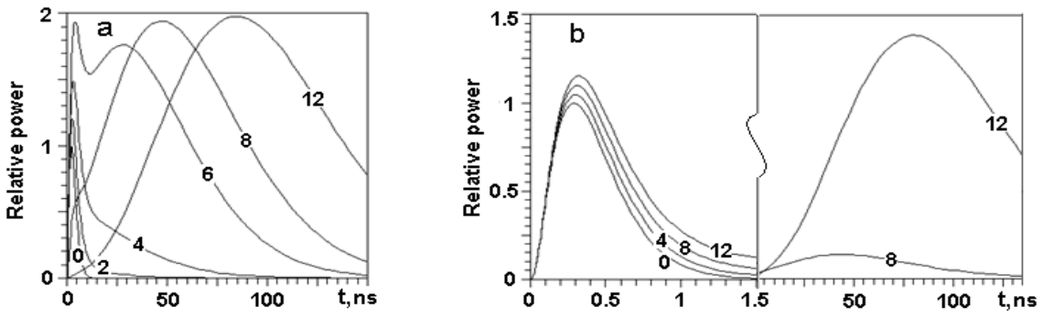

Fig. 8. Output Stokes pulse shapes for a), t_p = 4 ns (<τ) and G = 0(1), 2(1), 4(1), 6(1), 8(0.2), and 12(0.007), and b), for t_p = 0.5 ns (<<τ) and G = 0(1), 4(1), 8(1), and 12(1 at the first peak and 0.3 at the tail). LHS of b) is temporally stretched to show profiles.

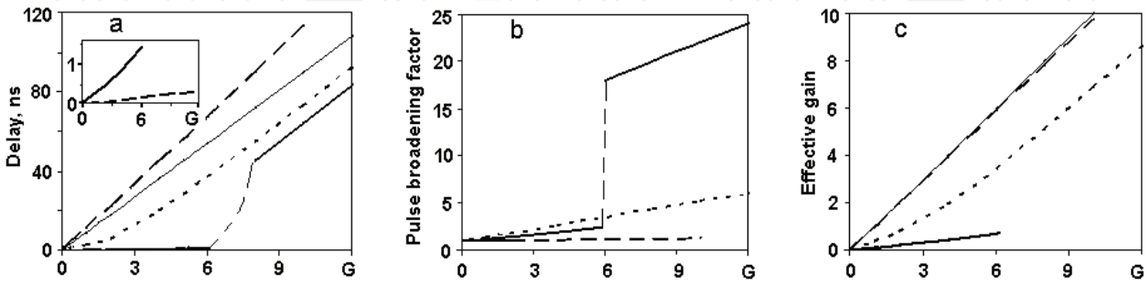

Fig. 9. Output Stokes pulse a), delay, b), broadening factor, and c), effective exponential gain at peak of output pulse vs gain G for pulse durations t_p = 200 (dashed), 18 (dotted), 4 (thick solid in the main graph and in the insert), and 0.5 ns (dashed in the inset). Thin solid lines in a) and c) are ΔT_d = 9G ns and G_{ef} = G dependencies respectively.

Figs 7 and 8 show the calculated relative output Stokes pulse powers, $P_S(t) = |E_S(t)|^2 S$ (S is the effective area of fiber–mode cross section), shapes, amplitudes and delays for four input pulse durations, t_p, and different G. Here the decay time, τ, of the hyper-sound wave in silica is taken to be $\tau = 18$ ns at a pump radiation wavelength ~1.55 μm. It should be emphasized that the decay time of the acoustic wave, which is determined by the viscosity of fused silica (Pinnow, 1970), is used in these calculations rather than the SBS spectral width. This is because the latter depends on intrinsic characteristics of the fiber (core/cladding design, doping type and concentration, numerical aperture, etc. and the ambient environment (mechanical, thermal and electromagnetic fields (see Sec. 3), all of which can result in substantial variation of the resonant Brillouin frequency, Ω_B. However they do not appreciably effect the viscosity of the medium.

It follows from Figs 7 and 8 that the induced delay of the output Stokes pulse, its duration and peak power, which is estimated to be $P_{S0}e^{Gef}$, where G_{ef} is the effective SBS exponential gain, in all cases increase with increase of G. Rates of these growths depend substantially on the ratio of pulse duration to acoustic wave decay time, t_p/τ, as shown in Fig. 9.

For a long input Stokes pulse, $t_p = 200$ ns that is $t_p/\tau = 200/18 >> 1$, the output pulse, on increase of G, remains similar in form (Fig. 7(a)), and is increasingly delayed following $\Delta T_d/G \cong 11$ ns as shown by the thick dashed line in Fig. 9(a). Additional calculations have shown that it may coincide with $\Delta T_d \cong \tau G/2 \cong 9G$ ns (shown by the thin solid line in Fig. 9(a)), but this happens only when $t_p/\tau \cong 2.5 \pm 0.5$ and >100. For $t_p/\tau < 2$ the growth of ΔT_d falls below the value $\Delta T_d \cong 9G$ ns. The duration of the output pulse compared to that of the input is slightly broadened with increase of G (see dashed line in Fig. 9(b)), and G_{ef} decreases very slightly compared to G (dashed line in Fig. 9(c)).

For $t_p = 18$ ns (Fig. 7(b)), that is $t_p/\tau = 1$, ΔT_d for the output pulse again increases with G though not linearly; at lower G (0 to ~2) with slope $\Delta T_d/G \cong 3$ ns, and at higher G (> 2) with slope $\Delta T_d/G \cong 9$ ns (dotted line in Fig. 9(a)). The pulse broadening in this case increases substantially with G, by a factor ≥ 5 at G > 10 (dotted line in Fig. 9(b)) and G_{ef} decreases notably, by a factor of ~3 at lower G to ~1.5 at G ≥ 10 (dotted line in Fig. 9(c)).

For the short pulses, $t_p \leq 4$ ns (Fig. 8), that is for $t_p/\tau < 1$, significant new features appear. For G < 4 the output pulses approximately retain their shape with only a slight increase of ΔT_d with G ($\Delta T_d/G \cong 0.1$-0.15 ns for $t_p = 4$ ns and $\Delta T_d/G \cong 0.03$ ns for $t_p = 0.5$ ns, as is shown in inset of Fig. 9(a), solid and dashed lines respectively). In both cases G_{ef} for the leading peak decreases substantially, by a factor ~10. For G between 4 and 6 there is substantial growth of the power in the tail of the pulses and for G > 8 the maximum of the pulse shifts to the tail (see Figs. 8(a) and 8(b)). This is because of the long decay of the acoustic wave excited by the short Stokes pulse interacting with the CW pump. The dependence of ΔT_d on G for G > 8 then follows the linear relation $\Delta T_d \cong (9G - 25)$ ns (thick solid line in Fig. 9(a)). The pulse broadening factor is then ~20 for $t_p = 4$ ns (solid line in Fig. 9(b) at G > 6) and ~200 for $t_p = 0.5$ ns.

It is interesting to note that analytical results presented in Figs. 7 and 8, which are obtained in the small signal limit, give dependencies of pulse delay and broadening on G quite similar to these obtained numerically both for long pulses, $t_p/\tau \cong 15$ and 5 in (Zhu et al, 2005), and for short pulses, $0.1 < t_p/\tau < 2$ in (Kalosha et al., 2006). There are however some quantitative differences, which are important to highlight. The numerical modelling in (Zhu et al., 2005) gives $\Delta T_d = \tau G/2$ dependence for $t_p/\tau \cong 15$, while calculations here predict this

only for t_p/τ in the region ~2.5±0.5, while for $t_p/\tau > 5$ the slope ΔT_d /G is a factor 1.2-1.3 steeper. Also the shape of the ΔT_d upon G dependence for $t_p/\tau \cong 5$ in ((Zhu et al, 2005)) is similar to that in these calculations but for $t_p/\tau \cong 1$. As to the numerical results presented in (Kalosha et al., 2006), the difference with findings here is most probably because all their results were obtained for an input Stokes power well above that for onset of pump depletion (input Stokes power is of 1 mW compared with pump power of ≤ 20 mW).

To understand the underlying nature of the behaviour described above consider through Eq. (28) the temporal and spectral characteristics of the complex dielectric function variation in the medium, $\Delta\varepsilon = (\partial\varepsilon/\partial\rho)\rho = \Delta\varepsilon' + i\Delta\varepsilon''$, induced by the interaction of the pump and Stokes signals; $\Delta\varepsilon(\omega)$ results in the SBS gain and $\Delta\varepsilon'(\omega)$ is responsible for modification of the refractive index, $\Delta n(\omega) \cong \Delta\varepsilon'(\omega)/2n_0$, of the medium, where n_0 is the refractive index of a medium without SBS. In the limit of small gain, G < 1, the Bessel function $I_0(x)$ in Eq. (28) may be set to unity, and analysis is greatly simplified. While this approximation does not allow us to describe gain narrowing of the SBS spectrum typical for higher G, it still captures reasonably well the trends in the temporal and spectral features of ρ, which determine those of the SBS gain and modified refractive index.

When $I_0(x) = 1$, the integral in Eq. (28) can be taken for $E_{S0}(t)$ given by Eq. (30). It results in the following analytic expression for $\rho(t)$,

$$\rho(t) = A\left\{\frac{2}{(2b-\tau)^2}\left[2\tau b\left(e^{-\frac{t}{\tau}} - e^{-\frac{t}{2b}}\right) + (2b-\tau)te^{-\frac{t}{2b}}\right]\right\}, \tag{29}$$

where $b = t_p/3.5$, and $A = -i\rho_0\frac{\partial\varepsilon}{\partial\rho}\frac{\Omega_B}{8\pi v^2}E_p E_S^*(0)$. The spectral characteristics of the acoustic wave amplitude follow from the Fourier transform of Eq.(31),

$$\rho(\omega) = A\sqrt{\frac{2}{\pi}}\frac{4\tau b}{(2b-\tau)^2}\left[\tau\frac{1+i\tau\omega}{1+(\tau\omega)^2} - 2b\frac{1+i2b\omega}{1+(2b\omega)^2}\right] + \sqrt{\frac{2}{\pi}}\frac{8b^2}{(2b-\tau)}\left[\frac{1+i4b\omega-(2b\omega)^2}{[1+(2b\omega)^2]^2}\right]. \tag{30}$$

The temporal dynamics of the induced acoustic wave amplitudes and their spectra for values of t_p/τ considered above are shown in Fig. 10 (the dynamics for t_p = 0.5 ns is not shown on the timescale of Fig. 10(a)). The curves in Fig. 10(a) represent different characteristic types of SBS interaction: curves 1 give an example of quasi-steady state interaction when $t_p/\tau >> 1$, curves 3 demonstrate transient type interaction when $t_p/\tau << 1$, and curves 2 are for an intermediate case when $t_p/\tau \cong 1$.

In the first case of a long Stokes pulse, that is $t_p/\tau >> 1$, the shape of the acoustic wave pulse shown in Fig. 10(a) as the solid curve 1 almost reproduces the shape of the input Stokes pulse (dotted curve 1). The spectrum of the excited acoustic wave in this case, Fig. 10(b), reproduces the spectrum of the input Stokes pulse, shown by the solid and dashed curves 1 respectively. These are both narrower than the Lorentzian-shaped spectrum corresponding to τ = 18 ns (dotted curve 5).

This is to be expected since Eq. (2) is in essence the equation for the amplitude of a driven damped oscillator; for such a system the spectrum of the induced oscillations is fully

determined by the spectrum of the driving force when it is narrower than the reciprocal decay time of the oscillator.

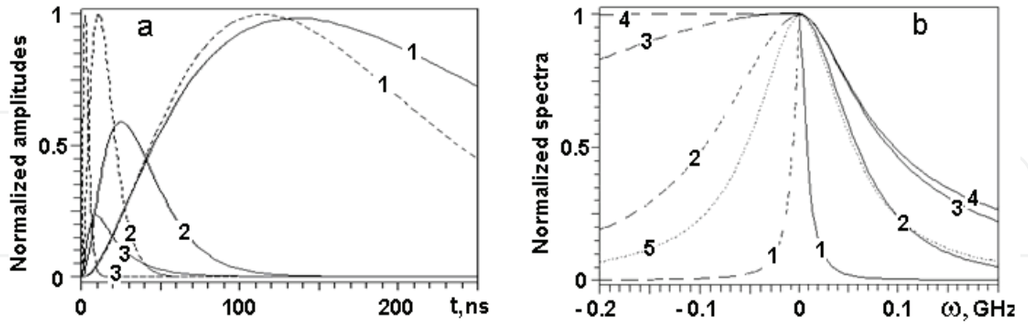

Fig. 10. a), Dynamics and b), spectra of the normalised acoustic wave amplitude (solid lines) for Stokes pulses of the shape given by Eq. (30) (dashed lines) with t_p = 200(1), 18(2), 4(3) and 0.5 ns(4), τ = 18 ns. The dotted line 5 in b), is the Lorentzian spectrum with τ = 18 ns. Curves in b) show half spectra of pulses at LHS and of corresponding medium's response at RHS.

In the case of shorter Stokes pulses, $t_p/\tau \leq 1$, (dashed curves 2 and 3 in Fig. 10(a)) the spectrum of the driving force, that is that of the input Stokes pulse, is broad band, (dashed curves 2 and 3 and also curve 4 for t_p = 0.5 ns pulse in Fig. 10(b)). As seen the dynamics of the medium's response (solid curves 2 and 3 in Fig. 10(a)) and its spectra (solid curves 2, 3 and 4 in Fig. 10(b)) differ substantially from those of the Stokes pulses and their spectra. In the temporal domain the maximum amplitude of the induced ρ(t) decreases with decrease of pulse duration and a long tail appears after a Stokes pulse, which decays exponentially with a decay time of τ. The spectra of ρ(t) in these cases are narrower, increasingly so for shorter pulses, than the spectra of the driving force (input Stokes pulse). Their width is then determined predominantly by the reciprocal decay time of the oscillator (dotted curve 5 in Fig. 10(b)) as is to be expected for a damped oscillator, which is driven by a broad-band force. Reduction of amplitude of the induced ρ(t) with decrease of pulse duration results in reduced amplitude of the output Stokes pulse and its effective G as shown in Fig. 9(c).
The imaginary part of $\rho(\omega)$ described by Eq. (13) gives the refractive index of the medium modified by the SBS interaction, $n(\omega) = n_0 + \Delta n(\omega) \cong n_0 + (\partial\varepsilon/\partial\rho)\rho(\omega)/2n_0$ and its corresponding group index, $n_g(\omega) = n_0 + \omega[d\Delta n(\omega)/d\omega]$ (Okawachi et al., 2005, Zhu et al., 2005). Spectra of the Stokes pulses and the group indices induced by these pulses are shown in Fig. 11 for the four different t_p/τ. It is important to remember (see section 3.2, Eqs (23) and (24)) that the group index profile is frequency shifted from the centre frequency of the Stokes pulse by $\sim 1.7 \cdot 10^4 \Omega_B$ and therefore has negligible effect on the Stokes pulse delay. In the literature on SL via SBS, it is assumed that their centre frequencies coincide. However even if this were so it is clear from Fig. 11 that the spectral width of a Stokes pulse is bigger than that of the SBS induced group index regardless of t_p/τ. As such, in this hypothetical case, while some, central, part of the input spectrum may experience a group delay, other parts of the spectrum will experience group advancement or neither delay or advancement (see Figs. 11(c) and 11(d)).

It therefore follows that regardless of the pulse length of the input Stokes pulse the pulse delays associated with SBS amplification of a Stokes pulse, as described above, cannot be attributed to SBS induced group delay. They are predominantly a consequence of the phenomenon of SBS build-up.

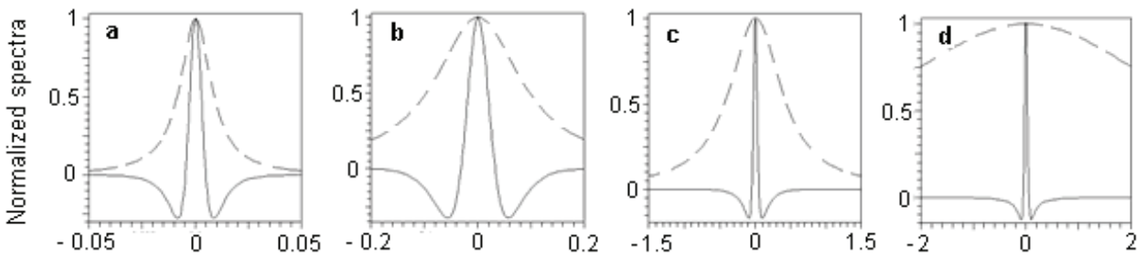

Fig. 11. Relation between the spectra of a Stokes pulse and of the group index induced by this pulse for t_p = 200 a), 18 b), 4 c), and 0.5 ns d). Horizontal scales are in GHz.

5. Conclusions

The results presented in this chapter raise the question of whether slow light, as first discussed in (Zeldovich, 1972), can be realised. To answer this recall the nature of the group delay effect. It is a linear phenomenon exhibited by a pulse propagating through a medium with normal dispersion of refractive index (Brillouin, 1960). The effect is greatly enhanced in the vicinity of a medium's resonance, which for a gain medium is normally dispersive. For SBS the maximum of this resonantly enhanced dispersion is centred around the Brillioun frequency, Ω_B, and it is all but negligible at the Stokes frequency. As such the acoustic resonance can have next to no effect in enhancing or modifying the natural group index in the medium for the Stokes signal. Consequently pulse delay associated with Stokes pulse induced SBS cannot be attributed to SBS induced group delay. It is predominantly a consequence of the phenomenon of SBS build-up, which arises from the inertia of the medium in responding to the optical fields. Also, spectral broadening of the pump radiation by any reasonable amount has next to no effect on the SBS spectral bandwidth of the excited acoustic wave in the medium, which is commonly believed to determine the SBS gain bandwidth (Thevenaz, 2008).

6. References

Agrawal, G. P. (2006). *Nonlinear Fiber Optics*, Academic Press, Boston.

Akhmanov, S. A., Drabovich, K. N., Sukhorukov, A. P. & Chirkin, A. S. (1971). Stimulated Raman scattering in a field of ultrashort light pulses, *Sov. Phys. JETP*, Vol. 32, 266-273.

Akhmanov, S. A., Dyakov, Yu. E. & Chirkin, A. S. (1988). *Introduction to Statistical Radiophysics and Optics*, Springer, Berlin.

Azuma, Y., Shibata, N., Horiguchi, T. & Tateda M. (1988). Wavelength dependence of Brillouin-gain spectra for single-mode fibres, *Electronics Letters*, Vol. 24, 250-252.

Basov, N.G., Ambartsumian, R.V., Zuev, V.S., Kryukov, P.G. & Letokhov, V.S. (1966). Nonlinear amplification of a light pulse. *Sov. Phys. JETP*, Vol. 23, 16-24.

Boyd, R. W. & Gauthier, D. J. (2002). "Slow" and "fast" light, *Progress in Optics*, Vol. 43, 497-530.

Brillouin, L. (1960). *Wave Propagation and Group Velocity*, Academic Press, New York.

Bronshtein, I. N. & Semendyayev, K. A. (1973). *A guide book to mathematics*. Verlag Harri Deutsch, Zurich.

Carman, R. L., Shimizu, F., Wang, C. S. & Bloembergen, N. (1970). Theory of Stokes pulse shapes in transient Raman scattering, *Phys. Rev. A*, Vol. 2, 60-72.

Cheng, A., Fok, M. P. & Shu, C. (2008). Wavelength-transparent, stimulated-Brillouin-scattering slow light using cross-gain-modulation-based wavelength converter and Brillouin fiber laser, *Optics Letters*, Vol. 33, 2596-2598.

Chin, S., Herraez, M. G. & Thevenaz, L. (2006). Zero-gain slow and fast light propagation in an optical fiber, *Optics Express*, Vol. 14, 10684-10692.

Gauthier, D. J. (2005). Slow light brings faster communications, *Physics World*, Vol. 18, 30-32.

Hau, L. V., Harris, S. E., Dutton, Z. & Behroozi, C. H. (1999). Light speed reduction to 17 meters per second in an ultracold atomic gas, *Nature*, Vol. 397, 594-596.

Heiman, D., Hamilton, D. S. & Hellwarth, R. W. (1979). Brillouin scattering measurements in optical glasses, *Phys. Rev*. Vol.19, 6583-6592.

Herraez, M. G., Song, K. Y. & Thevenaz, L. (2006). Arbitrary-bandwidth Brillouin slow light in optical fibers, *Opt. Express*, Vol. 14, 1395-1400.

Kalosha, V. P., Cheng, L. & Bao, X. (2006). Slow and fast light via SBS in optical fibers for short pulses and broadband pump, *Optics Express*, Vol. 14, 12693-12703.

Knight, J. C., Arriaga, J., Birks, T. A., Ortigosa-Blanch, A., Wadsworth, W. J. & Russel, P. St. (2000). Anomalous dispersion in photonic crystal fibre, *IEEE Photonics Technology Letters*, Vol. 12, 807-809.

Korn, G. A. & Korn, T. M. (1967). *Manual of mathematics*, McGraw-Hill, New York.

Kovalev, V. I. & Harrison, R. G. (2000). Observation of inhomogeneous spectral broadening of stimulated Brillouin scattering in an optical fiber, *Phys. Rev. Lett*. Vol. 85, 1879-1882.

Kovalev, V. I. & Harrison, R. G. (2002). Waveguide-induced inhomogeneous spectral broadening of stimulated Brillouin scattering in optical fiber, *Optics Letters,* Vol. 27, 2022-2024.

Kovalev, V. I. & Harrison, R. G. (2005). Temporally stable continuous-wave phase conjugation by stimulated Brillouin scattering in optical fiber with cavity feedback, *Optics Letters*, Vol. 30, 1375-1377.

Kovalev V. I. & Harrison, R. G. (2007). Threshold for stimulated Brillouin scattering in optical fiber, *Optics Express*, Vol. 15, 17625-17630.

Kovalev, V. I., Harrison, R. G., Knight, J. C. & Kotova, N. E. (2008). Waveguide induced spectral bandwidth enhancement of slow light group index caused by stimulated Brillouin scattering in optical fiber," *Laser and Particle Beams,* Vol. 26, 319-322.

Kovalev, V. I., Kotova, N. E. & Harrison, R. G. (2009). Effect of acoustic wave inertia and its implication to slow light via stimulated Brillouin scattering in an extended medium, *Optics Express*, Vol.17, 2826-2833.

Kroll, N. (1965). Excitation of hypersonic vibrations by means of photoelastic coupling of high-intensity light waves to elastic waves, *J. Appl. Phys*. Vol. 36, 34-43.

Le Floch, S. & Cambon, P. (2003). Study of Brillouin gain spectrum in standard single-mode fiber at low temperatures (1.4-370 K) and high hydrostatic pressures (1-250 bars), *Optics Communications*, Vol. 219, 395-410.

Lu, Z., Dong, Y. & Li, Q. (2007). Slow light in multi-line Brillouin gain spectrum, *Optics Express*, Vol. 15, 1871-1877.

Minardo, A., Bernini, R. & Zeni, L. (2006). Low distortion Brillouin slow light in optical fibers using AM modulation, *Optics Express*, Vol. 14, 5866-5876.

Okawachi, Y., Bigelow, M. S., Sharping, J. E., Zu, Z., Schweinsberg, A., Gauthier, D. J., Boyd, R. W. & Gaeta, A. L. (2005). Tunable all-optical delays via Brillouin slow light in an optical fiber, *Phys. Rev. Lett.* Vol. 94, 153902.

Pant, R., Stenner, M. D., Neifeld, M. A. & Gauthier, D. J. (2008). Optimal pump profile designs for broadband SBS-based slow light systems, *Optics Express*, Vol. 16, 2764-2777.

Pinnow, D. A. (1970). Guide lines for the selection of acoustooptic materials, *IEEE J. Quantum Electron.* Vol. QE-6, 223-238.

Pohl D. & Kaiser, W. (1970). Time-resolved investigations of stimulated Brillouin scattering in transparent and absorbing media: Determination of phonon lifetimes, *Phys. Rev. B,* Vol.1, 31-43.

Ren L. & Tomita, Y. (2008). Reducing group-velocity-dispersion-dependent broadening of stimulated Brillouin scattering slow light in an optical fiber by use of a single pump laser, *J. Opt. Soc. Am. B*, vol. 25, 741-746.

Sakamoto, T., Yamamoto, T., Shiraki, K. & Kurashima, T. (2008). Low distortion slow light in flat Brillouin gain spectrum by using optical frequency comb, *Optics Express*, Vol. 16, 8026-8032.

Schneider, T., Junker, M. & Lauterbach, K.-U. (2006). Potential ultra wide slow-light bandwidth enhancement, *Optics Express*, Vol. 14, 11082-11087.

Schneider, T., Henker, R., Lauterbach, K.-U. & Junker, M. (2008). Distortion reduction in Slow Light systems based on stimulated Brillouin scattering, *Optics Express*, Vol. 16, 8280-8285.

Shi, Z., Pant, R., Zhu, Z., Stenner, M. D., Neifeld, M. A., Gauthier, D. J. & Boyd, R. W. (2007). Design of a tunable time-delay element using multiple gain lines for increased fractional delay with high data fidelity, *Optics Letters*, Vol. 32, 1986-1988.

Shibata, N., Waarts, R. G. & Braun R. P. (1987). Brillouin gain spectra for single-mode fibers having pure-silica GeO_2-doped, and P_2O_5-doped cores, *Optics Letters*, Vol. 12, 269-271.

Shibata, N., Okamoto, K. & Azuma Y. (1989). Longitudinal acoustic modes and Brillouin-gain spectra for GeO_2-doped-core single-mode fibers, *JOSA B*, Vol. 6, 1167-1174.

Shiraki, K., Ohashi, M. & Tateda, M. (1995). Suppression of stimulated Brillouin scattering in a fiber by changing the core radius, *Electronics Letters*, Vol. 31, 668-669.

Shumakher, E., Orbach, N., Nevet, A., Dahan, D. & Eisenstein, G. (2006). On the balance between delay, bandwidth and signal distortion in slow light systems based on stimulated Brillouin scattering in optical fibers, *Optics Express*, Vol. 14, 5877-5884.

Song, K. Y., Herraez, M. G. & Thevenaz, L. (2005). Gain-assisted pulse advancement using single and double Brillouin gain peaks in optical fibers, *Optics Express*, Vol. 13, 9758-9765.

Song K. Y. & Hotate, K. (2007). 25 GHz bandwidth Brillouin slow light in optical fibers, Optics Letters, Vol. 32, 217-219.

Stenner, M. D., Neifeld, M. A., Zu, Z., Dawes, A. M. C. & Gauthier D. J. (2005). Distortion management in slow-light pulse delay, *Opt. Express*, Vol. 13, 9995-10002.

Thevenaz, L. (2008). Slow and fast light in optical fibres, *Nature Photonics*, Vol. 2, 474-481.

Tkach, R. W., Chraplyvy, A. R. & Derosier, R. M. (1986). Spontaneous Brillouin scattering for single-mode optical-fibre characterisation, *Electronics Letters*, Vol. 22, 1011-1013.

Tsun, T.-O., Wada, A., Sakai, T. & Yamauchi, R. (1992). Novel method using wight spectral probe signals to measure Brillouin gain spectra of pure silica core fibres, *Electronics Letters*, Vol. 28, 247-249.

Wang, S., Ren, L., Liu, Y. & Tomita, Y. (2008). Zero-broadening SBS slow light propagation in an optical fiber using two broadband pump beams, *Optics Express*, Vol. 16, 8067-8076.

Yi, L., Zhan, L., Hu, W. & Xia, Y. (2007). Delay of broadband signals using slow light in stimulated Brillouin scattering with phase-modulated pump, *IEEE Photon. Technol. Letters,* Vol. 19, 619-621.

Yoshizawa, N., Horiguchi, T. & Kurashima, T. (1991). Proposal for stimulated Brillouin scattering suppression by fibre cabling, *Electronics Letters*,Vol. 27, 1100-1101.

Yoshizawa, N. & Imai, T. (1993). Stimulated Brillouin scattering suppression by means of applying strain distribution to fiber with cabling, *Journal of Lightwave Technology*, Vol. 11, 1518-1522.

Zadok, A., Eyal, A. & Tur, M. (2006). Extended delay of broadband signals in stimulated Brillouin scattering slow light using synthesized pump chirp, *Optics Express*, Vol. 14, 8498-8505.

Zeldovich, B. Ya. (1972). Time of establishment of stationary regime of stimulated light scattering, *JETP Lett*. Vol. 15, 158-159.

Zeldovich, B. Ya., Pilipetskii N. F. & Shkunov V. V. (1985). *Principles of phase conjugation*, Springer Verlag, Berlin.

Zhang, B., Yan, L., Fazal, I., Zhang, L., Willner, A. E., Zhu, Z. & Gauthier, D. J. (2007)-1. Slow light on Gbit/s differential-shift-keying signals, *Optics Express*, Vol. 15, 1878-1883.

Zhang, B., Zhang, L., Yan, L.-S., Fazal, I., Yang, J.-Y. & Willner, A. E. (2007)-2. Continuously-tunable, bit-rate variable OTDM using broadband SBS slow-light delay line, *Optics Express*, Vol. 15, 8317-8322.

Zhu, Z., Gauthier, D. J., Okawachi, Y., Sharping, J. E., Gaeta, A. L., Boyd, R. W. & Willner, A. E. (2005). Numerical study of all-optical slow-light delays via stimulated Brillouin scattering in an optical fiber, *J. Opt. Soc. Am. B*, Vol, 22, 2378-2384.

Zhu Z. & Gauthier, D. J. (2006). Nearly transparent SBS slow light in an optical fiber, *Optics Express*, Vol. 14, 7238-7245.

Zhu, Z., Dawes, A. M. C., Gauthier, D. J., Zhang, L. & Willner, A. E. (2007). Broadband SBS slow light in an optical fiber, *J. Lightwave Technol*. Vol. 25, 201-206.

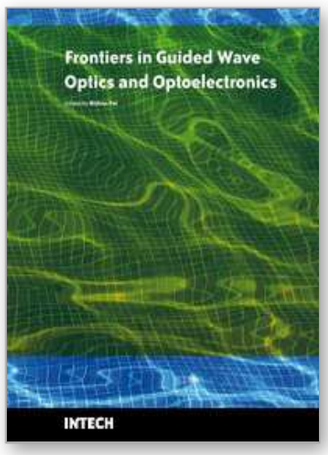

Frontiers in Guided Wave Optics and Optoelectronics

Edited by Bishnu Pal

ISBN 978-953-7619-82-4
Hard cover, 674 pages
Publisher InTech
Published online 01, February, 2010
Published in print edition February, 2010

As the editor, I feel extremely happy to present to the readers such a rich collection of chapters authored/co-authored by a large number of experts from around the world covering the broad field of guided wave optics and optoelectronics. Most of the chapters are state-of-the-art on respective topics or areas that are emerging. Several authors narrated technological challenges in a lucid manner, which was possible because of individual expertise of the authors in their own subject specialties. I have no doubt that this book will be useful to graduate students, teachers, researchers, and practicing engineers and technologists and that they would love to have it on their book shelves for ready reference at any time.

InTech Europe
University Campus STeP Ri
Slavka Krautzeka 83/A
51000 Rijeka, Croatia
Phone: +385 (51) 770 447
Fax: +385 (51) 686 166
www.intechopen.com

InTech China
Unit 405, Office Block, Hotel Equatorial Shanghai
No.65, Yan An Road (West), Shanghai, 200040, China
中国上海市延安西路65号上海国际贵都大饭店办公楼405单元
Phone: +86-21-62489820
Fax: +86-21-62489821

IntechOpen